Rev Anal Chem 31 (2012): 7–14 © 2012 by Walter de Gruyter • Berlin • Boston. DOI 10.1515/revac-2011-0031

On-chip redox cycling techniques for electrochemical detection

Enno Kätelhön[1,2] and Bernhard Wolfrum[1,2,*]

[1] Institute of Bioelectronics (ICS-8/PGI-8), Forschungszentrum Jülich GmbH, 52425 Jülich, Germany, e-mail: b.wolfrum@fz-juelich.de
[2] JARA, Fundamentals of Future Information Technology, Forschungszentrum Jülich GmbH, 52425 Jülich, Germany

* Corresponding author

Abstract

During the last two decades, redox cycling techniques have evolved as a promising technique for the electrochemical detection of molecules that can undergo subsequent redox reactions. In particular, chip-based techniques received growing attention due to the option of parallel fabrication and easy integration into lab-on-a-chip devices. In here, we provide a review on current implementations of on-chip redox cycling sensors. Advantages and limitations of various approaches are discussed with regard to their fabrication process and performance.

Keywords: electrochemical sensors; interdigitated arrays; nanocavity sensors; nanofluidic sensors; redox cycling.

Introduction

Electrochemical techniques are used in a variety of scientific disciplines ranging from fundamental research on chemical reactions to applications such as fuel cells, solar cells, or sensors for operation in biological or environmental analysis. These sensors utilize certain surface reactions at interfaces between an electrode and a liquid or gaseous sample that link chemical reactions to electrical currents. Measured currents then allow conclusions regarding analyte concentrations or can be studied in order to gain insight into chemical reactions at the device. In most applications, a set of electrode probes that feature inert or chemically modified electrode surfaces is used in liquid environments. During the measurement, the electrodes are immersed into the sample solution and then biased to a well-defined potential with regard to the solution's potential, which is typically defined via a reference electrode. Thus, chemical reactions of certain molecules may be enabled at the electrode surfaces, while electrode currents are measured. The detected currents, which are usually recorded as a function of the applied voltage as well as the applied voltage's chronological sequence, may then provide information on various characteristics of the sample, such as molecular reactions and diffusion characteristics. Most commonly, such investigations are performed using amperometry, a method in which a working electrode is biased to a constant potential that is suitable to oxidize or reduce the species under investigation, while a reference electrode or a set of a reference electrode and an auxiliary electrode define the solution potential. The current at the working electrode is then proportional to the number of molecules that react per unit time at the working electrode and can, hence, be used to calculate the analyte concentration. However, amperometry offers little selectivity as a wide range of molecules can participate in the redox reactions. A more detailed analysis can be done via the method of cyclic voltammetry (CV). Here, the electrode potential of the working electrode is repeatedly swept from an oxidizing to a reducing potential in a triangular fashion at a low frequency, while the electrode current is recorded (Nicholson and Shain 1964, Nicholson 1965). By this means, a more specific analysis can be performed, as not only the current but also the current as a function of the applied voltage is recorded. Hence, the analysis can also provide information on the analyte redox potential as well as its diffusive behavior. However, even though the CV approach can be used in a wide field of applications, it holds the disadvantage that the overall current and equally the detection limit are always restricted by the mass transfer of analyte molecules toward the electrode surface. This limitation can be overcome to some extent by the method of fast-scan cyclic voltammetry (FSCV), which performs CV measurements at frequencies in the kHz (Howell and Wightman 1984) or even MHz range (Amatore et al. 2000). The sensitivity is then no longer limited by the mass transfer as long as the cycling frequency dominates diffusion and analyte molecules can undergo repeated redox reactions. Fast scan rates also lead to an increased selectivity because mostly, redox-active molecules, i.e., molecules that can undergo repeated redox reactions, are detected. Even though high-capacitive background currents and electrode fouling remain as challenges in current research (Swamy and Venton 2007, Keithley et al. 2011), today, FSCV is a powerful technique used for the detection and investigation of neurotransmitter release of biological cells (Wightman et al. 1991, Wightman 2006, Bledsoe et al. 2009, Hernández and Shizgal 2009, Kraft et al. 2009, Zachek et al. 2010).

Many issues regarding sensitivity and selectivity of electrochemical sensors can be eliminated by the application of multi-electrode systems that enable redox cycling (Rassaei et al. 2011). In redox cycling, a second working electrode is placed in close proximity to the first electrode, while both electrodes are individually biased to potentials above and below the redox potential of a reversible redox couple. Driven by molecular diffusion, redox-active molecules then participate in repeated redox reactions between the electrodes, while a charge is transferred from one electrode to the other whenever a molecule subsequently reacts at both electrodes (see Figure 1). These charges can then be detected as a net

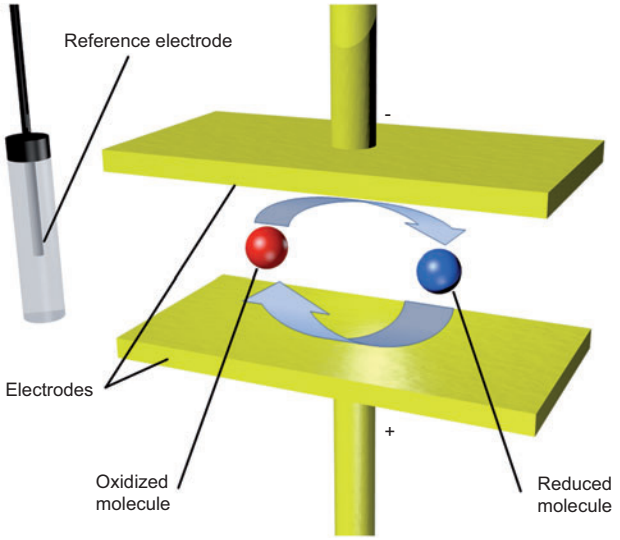

Figure 1 Illustration of the redox cycling mechanism. The sketch depicts the oxidizing and the reducing electrode as well as a reference electrode. Redox-active molecules are indicated by the two spheres, while the red and the blue colorings represent the oxidized and reduced molecule states, respectively.

current across the electrode gap. Today, redox cycling sensors are used in a wide field of applications (Niwa 1995). The large signal amplification and the ability to integrate arrays of microscopic redox cycling sensors at a high density make the technique interesting for detection of localized events, such as neurotransmitter release. Hence, redox cycling sensors may evolve to a tool for on-chip neuroscience experiments.

Redox cycling

The sensing performance of redox cycling devices is mainly determined by the device geometry. Amplification scales with the inter-electrode distance h, as the average time T_s a molecule requires for the shuttling from one electrode to the other highly depends on this distance h. The shuttling time T_s for a plane-parallel arrangement can be calculated using a general solution of the one-dimensional diffusion equation:

$$\Delta x^2 = 2D\Delta t$$

(D describes the diffusion constant). Substituting h for the average spatial displacement Δx and T_s for the average time interval Δt this displacement takes, we obtain:

$$T_s = \frac{h^2}{2D}$$

Utilizing T_s, one can now calculate the average cycling current I_{cycl} across the electrode gap, which is caused by a single molecule that is located in between the electrodes and that can transfer n elementary charges e_0:

$$I_{cycl} = \frac{ne_0}{2T_s} = \frac{ne_0 D}{h^2},$$

(Fan and Bard 1995, Wolfrum et al. 2008). In order to quantify the redox cycling amplification of the electrochemical current, different methods can be employed. The simplest approach is given by dividing the current of the working electrode in redox-cycling mode by the current obtained when the same device is used without redox cycling (i.e., only one working electrode is connected). However, this definition can be misleading, as the single-electrode current is strongly dependent on the coupling of the sensor and the bulk reservoir. For example, consider the extreme case of a redox cycling device within a small confined box: any such device would yield a finite steady state current while operating in redox cycling mode. However, in single-electrode mode, the resulting current will approach zero after all molecules have been either oxidized or reduced to the same state in the box system. Thus, with the definition above, the amplification factor of all strongly confined redox cycling systems will tend toward infinity. Although the confinement can be an important parameter of the device, we believe that it should rather be addressed in terms of efficiency instead of the amplification factor as we will discuss below. Another, and for concentration sensing, more useful, way of defining amplification can be obtained by dividing I_{cycl} by the current that would be expected from a microelectrode I_{me} of the same size due to radial diffusion (Wolfrum et al. 2008). For illustration, we calculated the current of an ideal redox cycling device with two plane-parallel opposing electrodes at a separation of 50 nm and compared this to the result for a single microdisk electrode of the same size as introduced by Shoup and Szabo (1982):

$$\frac{I_{me}}{4nFDrc_0} = f(\tau)$$

Using the definitions:

$$\tau = \frac{4Dt}{r^2}$$

and

$$f(\tau) = 0.7854 + 0.8862\tau^{-1/2} + 0.2146e^{-0.7823\tau^{-1/2}}$$

(r represents the radius of the electrode and F the Faraday constant). By dividing the two currents, we determined the amplification factor as a function of time as well as a function of the electrode radius r. The corresponding plots are shown in Figure 2. Using this definition, even at steady state, the amplification factor does not reach infinity but stays in the range of three orders of magnitude for a 50-µm radius electrode. From Figure 2B, we see that the amplification factor strongly increases for larger electrodes that approach steady-state values. Hence, the use of redox cycling in amperometric concentration sensing is particularly effective.

Another important design feature of redox cycling sensors is the degree to which analyte molecules are confined in between the electrodes. If a sensor design provides an easy access to the inter-electrode space from the bulk solution, sensors show a fast response to fluctuations in concentration

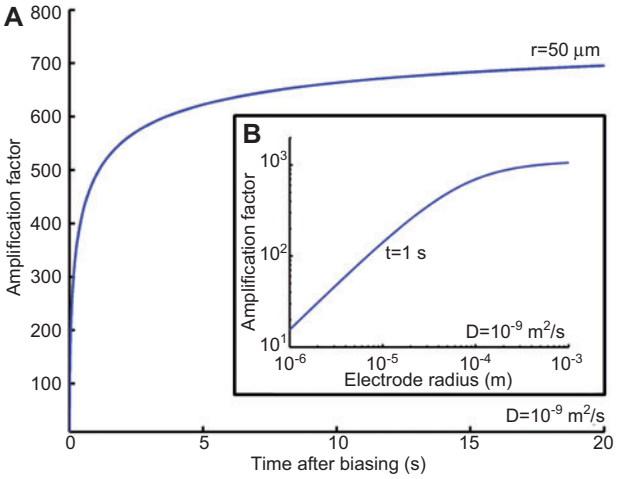

Figure 2 Amplification by the redox cycling effect. The presented plots picture the analytically determined amplification factors of the Faradaic currents obtained from a redox cycling sensor compared to a single disk electrode of equal size. (A) Presents the amplification as a function of the time passed since the electrode was biased for an electrode radius of 50 µm. (B) Shows the amplification at t=1 s as a function of the electrode radius.

of the analyte. However, the average number of redox cycles that each molecule performs inside the sensor is lower compared to more enclosed designs. This effect is insignificant for most concentration sensing applications, as the net number of molecules inside the sensor remains unaffected. Nevertheless, for certain concentration measurements or spectroscopic applications, it is desirable that each single molecule performs a large number of subsequent cycles. Examples are given by the detection of the "recyclable" molecule dopamine in the presence of ascorbic acid, which does not participate in subsequent redox reactions (Wolfrum et al. 2008) or the application of redox cycling sensors in adsorption spectroscopy as described by Singh et al. (2011).

The degree of confinement is highly dependent on the geometry of the surrounding space that is open for diffusion and, hence, depends on a variety of different design features. One approach to define a key number that is related to these features is given by the collection efficiency η. It is usually defined as the ratio of the currents I_{gen} and I_{col} at the generating and collecting electrodes (Bard et al. 1986, Niwa et al. 1990) and can be calculated as follows:

$$\eta=\frac{I_{col}}{I_{gen}}.$$

Even though this definition is very illustrative, its use can be problematic due to the experimental factors affecting η. The measured value is well dependent on the ratio of oxidized and reduced analyte molecules in the bulk solution, as potentially not only molecules that were generated at the generator contribute to the current at the collector and vice versa. In addition, the concept does rely on temporal aspects of the redox cycling itself. If the sensor impacts the analyte concentration in its immediate surroundings or forms a wide depletion layer of molecules that can react at the generator, collection efficiency will be time-dependent. In order to avoid these issues, two additional criteria for the experimental determination of η can be introduced: First, the experimentalist assures that the solution only contains analyte molecules of one oxidation state at the beginning of the experiment. This can be achieved via an additional macroscopic electrode in the bulk solution, for example. Second, measurements should be performed after the system comes to stationary conditions in currents and concentration distribution. As we focus on on-chip sensors, the access to the considered sensors is typically very small. In analog to microelectrodes, mass transfer toward the sensor is therefore affected by radial diffusion. Hence, mass transfer and Faradaic currents will equally converge to a steady-state value that can be measured (Shoup and Szabo 1982).

Off-chip implementations of redox cycling sensors

First redox cycling experiments were performed in the field of thin-film electrochemistry. During the mid-1960s, the group of Reilley used a micrometer electrode that was positioned in close proximity to an electrically conducting anvil, while the inter-electrode distance could be adjusted via a micrometer spindle (Anderson and Reilley 1965, Oglesby et al. 1965). Furthermore, both electrodes could be biased individually, and the current across the gap could be measured, hence, allowing confined redox reactions in between the electrodes. By this means, detailed studies of the redox reactions of the Fe(II)–Fe(III) and the quinone-hydroquinone redox couples were enabled.

During the 1980s, other fields of application arose. Among the off-chip techniques, scanning electrochemical microscopy (SECM) evolved as one of the most important methods. This technique was first pioneered by the groups of Bard and Engstrom (Engstrom et al. 1986, 1987, Liu et al. 1986, Bard et al. 1989, Fan and Bard 1995) and later advanced by a variety of other groups. Analog to a scanning tunneling microscope (STM), this approach utilizes a microprobe that scans the sample surface. However, contrasting STM measurements, a microelectrode is employed instead of a needle, and the sample is immersed in solution. During the measurement, redox cycling can be enabled in between the electrode tip and the substrate. In case redox cycling occurs, this method is usually referred to as positive feedback mode. It allows the mapping of surfaces in detail with regard to their topography and chemical reactivity (Barker et al. 1999, Mirkin and Horrocks 2000). In 1995, Fan and Bard employed this approach for the detection of single molecules (Fan and Bard 1995).

Even though advances in thin-film electrochemistry and SECM paved the way for the development of on-chip redox cycling techniques, in the following, this review will solely focus on on-chip approaches.

Interdigitated arrays

Interdigitated array sensors (IDAs) represent a group of on-chip electrochemical sensors that utilize the redox cycling technique. IDAs were initially described by Sanderson and Anderson in 1985 and then further studied by other groups with regard to miniaturization and applicability for the detection of various redox-active species (Sanderson and Anderson 1985, Chidsey et al. 1986, Feldman and Murray 1986, Aoki et al. 1988). Today, IDAs are commonly used on-chip redox cycling sensors and are employed in a wide range of applications.

A single IDA sensor consists of two coplanar electrodes that feature comb-like shapes and are arranged in an interdigitated fashion (see Figure 3). Electrodes are typically fabricated from inert metals and exhibit inter-electrode distances from the nanometer up to the micron scale (Ueno et al. 2005).

In most sensing applications, IDAs are operated in amperometric or cyclic voltammetry mode. During amperometric operation, electrodes are biased individually to potentials above and below the redox potential of the species under investigation, hence, enabling redox cycling in between the electrodes. The overall current across the electrode gap is then measured, and conclusions regarding the analyte concentration can be drawn. In contrast to that, in CV mode one electrode remains biased to a potential below or above the redox potential, while the other is repeatedly swept from an oxidizing to a reducing potential and vice versa. During the measurement, the current at the constantly biased electrode is recorded. By this means, cyclic voltammograms are obtained that are mainly limited by the diffusive shuttling of reactive molecules in between the electrodes instead of the diffusive mass transfer from the bulk solution toward the electrode. This mode of data acquisition offers an additional insight into molecular kinetics at the electrode surface in a trade off for a better temporal resolution in amperometric operation.

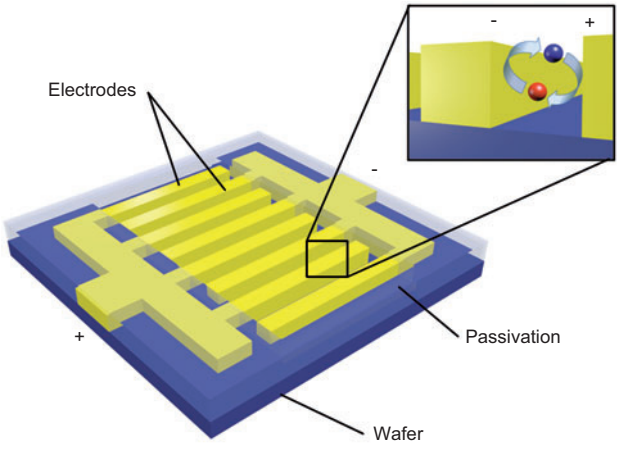

Figure 3 Illustration of an interdigitated array sensor. Both electrodes can be biased individually via feed lines that are covered under a thin passivation layer. Inset: Redox cycling occurs in between the electrodes. Oxidized molecules are indicated by a red sphere, reduced molecules by a blue sphere.

Besides their good measurement capabilities, the wide use of IDAs is also based on their comparable simple and cheap fabrication process in comparison to other microelectrode-based approaches. Simple sensor designs can be fabricated via a single lateral structuring step using microfabrication techniques such as optical lithography or nanoimprint lithography for parallelized production or electron beam lithography for prototyping. This results in a quick and inexpensive fabrication of nano-scaled devices. Regarding larger structures, printed electronics evolve as a cheap alternative. However, IDAs also exhibit certain disadvantages. First, the amplification by the redox cycling effect is always limited by the distance between the electrodes, which itself is limited by the structuring method applied. Therefore, high amplification can only be achieved by sets of nanoelectrodes that were produced via more complex fabrication methods. Also, nanoelectrodes exhibit poorer stability at decreasing structure sizes, which results in shorter disabilities in sensing applications. Second, the redox cycling efficiency does not reach the level achieved by confined redox cycling approaches, as a significant part of the analyte molecules does not participate in repeated redox cycling but diffuse away.

Recent developments related to the design of IDAs mainly focus on the increase of sensitivity by optimizing the senor geometries toward more confined redox cycling (Goluch et al. 2009). During the last decade, various methods were introduced that increase the aspect ratio of the interdigitated electrodes for better redox cycling efficiency (Honda et al. 2003, Kim et al. 2004, Dam et al. 2007). Furthermore, performance was increased significantly by scaling the inter-electrode distance down to sizes of 30 nm in IDAs or below 4 nm in a single nanogap (Ueno et al. 2005, McCarty et al. 2010). New developments aim for advanced on-chip signal amplification or high-throughput processing based on addressable microarrays (Ino et al. 2011, Takeda et al. 2011, Zhu et al. 2011) and complementary metal oxide semiconductor (CMOS) technology (Zhu and Ahn 2006, Zhan et al. 2007, Huang and Lu 2010).

Pore-based approaches

A different group of on-chip redox cycling sensors is given by pore-based designs. In contrast to IDAs, which feature electrodes that are positioned in a coplanar fashion on the wafer surface, pore-based designs utilize electrodes that are aligned in parallel to each other and the wafer surface. The sensors consist of a stack of two or more electrodes that are separated by insulating layers for the option of individual biasing. Diffusive access to a bulk reservoir is enabled via small openings in the form of pores that interpenetrate the stack (see Figure 4). Hence, the inter-electrode distance is no longer limited by the lateral resolution of the structuring method, but by the minimal thickness of the intermediate layer that is still sufficient for electrical isolation. In that way, the inter-electrode distance and, thus, the redox cycling amplification can be enhanced significantly, even though the overall active surface of the sensor is smaller in comparison to many other

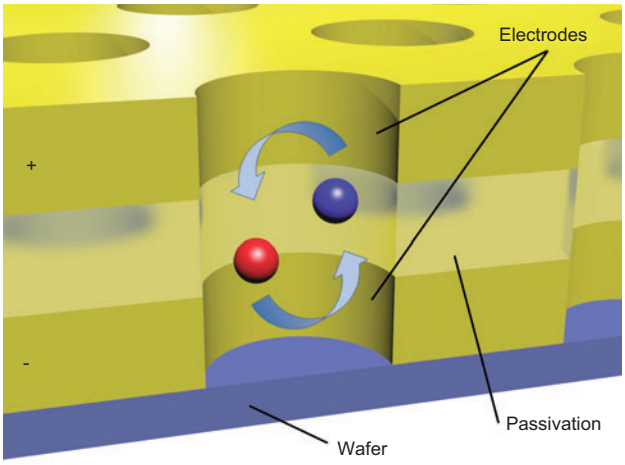

Figure 4 Illustration of a pore-based redox cycling sensor. Two porous metal electrodes are separated by an insulating layer. Redox-active molecules are indicated by the two colored spheres, whereas different colors represent different oxidation states.

sensor designs. Sensitivity in terms of the ratio of Faradaic current per sensor area can be improved further by scaling pore size and electrode spacing down, as the overall available electrode surface is mostly defined via the pore outline and density. Owing to their short-access-channel design, open-pore sensors are strongly coupled to the reservoir via molecular diffusion. This coupling increases the sensor's response characteristics to rapid concentration fluctuations making them especially suitable for time-resolved sensing applications. However, good coupling also leads to low degrees of confinement of the molecules inside the sensor pores and equally lowers redox cycling efficiency and amplification. As the coupling can be tuned via the aspect ratio of the pore dimensions, there is always a trade off between temporal resolution and redox cycling efficiency.

During the last 15 years, various approaches to technical implementations of pore-based sensors have been described. In 1999, Henry and Fritsch introduced devices that feature stacks of gold electrodes separated by insulating polyimide layers (Henry and Fritsch 1999a,b). Each sensor is characterized by a single, several micron wide opening that is etched perpendicularly into the stack in order to enable diffusive access to the bulk reservoir. In operation, electrodes are biased individually to facilitate redox cycling-enhanced electrochemical detection. By this means, dopamine concentrations as low as 2 µM were detected at micron-scaled sensors featuring inter-electrode distances of about 4 µm (Vandaveer et al. 2003). Another approach was introduced by collaboration between the groups of Spatz, Stelzle, and Schuhmann in 2006. In contrast to the work by Henry and Fritsch, here, electrode stacks do not feature only a single pore but are porous themselves (Neugebauer et al. 2006, 2008, Lohmüller et al. 2008). Unlike the formerly described sensors, structures are obtained via a bottom-up process. During fabrication, self-aligning nanoparticles are first disposed over the wafer surface and later utilized as a shadow mask in a lift-off process. By this means, dense patterns of pores were obtained that featured pore sizes down to 330 nm at an average spacing of about 650 nm. This method allows distinctly higher densities of active surface area compared to conventional top-down pore-based approaches and, hence, an increased redox cycling performance. An alternative bottom-up approach to the fabrication of pore-based redox cycling sensors makes use of nanoporous aluminum oxide templates (Hüske and Wolfrum 2011). Aluminum is deposited directly onto an electrode-insulator-electrode stack and anodized on spot, generating nanoscaled pores that form self-aligned in a hexagonal pattern. The porous alumina layer is then used as a shadow mask for reactive ion etching, thus, transferring the structure of the porous aluminum into the stack. This approach aims to scale down pore sizes and interpore spacings in a large-scale fabrication process without the use of electron beam or focused ion beam patterning.

Nanocavity devices

Nanocavity sensors (also referred to as "nanofluidic electrochemical sensors") currently represent the most spatially confined redox cycling technique on-chip. First, sensors were fabricated in the group of Lemay in 2007 and tested in various fields of application soon after (Zevenbergen et al. 2007, Wolfrum et al. 2008). During the fabrication process, a laterally aligned stack of a micron-sized bottom electrode, a thin sacrificial layer, and a second top electrode are deposited on the wafer surface and subsequently buried under a mechanically stable passivation layer. Afterwards, a small opening is etched into the passivation in order to enable fluidic access to the sacrificial layer. This layer is then removed using an anisotropic etch, hence, forming a cavity that separates the top and bottom electrode. Similar to pore-based approaches, the inter-electrode distance is defined by the layer thickness of a deposited layer instead of a lateral structuring method; however, compared to formerly introduced methods, significantly larger opposing electrode surfaces can be produced with this technology. In operation, both electrodes are biased individually for redox cycling through additional feed lines (see Figure 5). Diffusive access to the bulk reservoir is enabled via the opening in the passivation that formerly provided access to the sacrificial layer.

The central advantage of nanocavity sensors is the strong signal amplification in combination with high redox cycling efficiency, which is due to the large surface areas that are obtained at nano-scaled inter-electrode distances. This combination allows sensitivity down to the ultimate limit: Zevenbergen et al. recently demonstrated the electrochemical detection of a single molecule inside a nanofluidic cavity (Zevenbergen et al. 2011). In their experiment, each individual molecule contributed with an average electrochemical current of 78 fA to the overall current. Although sharp transitions due to molecule fluctuations were not observed because of the limited bandwidth, the results nicely demonstrate the possibilities for single molecule studies using on-chip electrochemical redox cycling amplification. Other

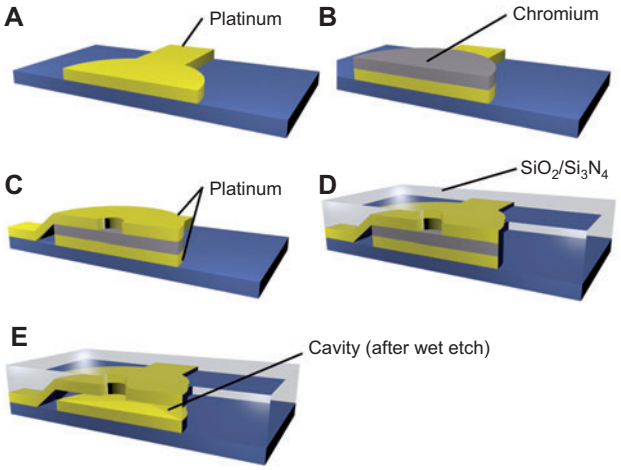

Figure 5 Illustration of the fabrication process of a nanocavity redox cycling sensor in a cross-section view. The sketch shows the individual production steps, i.e., the deposition of the bottom electrode (A), the sacrificial layer (B), the top electrode (C), and the passivation layer after the anisotropic etch (D). The last illustration depicts the final sensor after the removal of the sacrificial layer (E).

advantages of nanocavity devices include the applicability in spectroscopic methods. In 2009, the same group introduced the method of electrochemical correlation spectroscopy (ECS), which determines the fluctuations in the number of redox-active molecules within a given volume (Zevenbergen et al. 2009a) and exhibits great potential for the in-depth investigation of adsorption and desorption effects. Another application is given by the characterization of fast electron-transfer kinetics inside nanofluidic channels (Zevenbergen et al. 2009b). Design-related limitations mostly apply to the sensor response to rapid concentration fluctuations. Owing to the sensor's comparable high degree of confinement inside the cavity, diffusive coupling between the analyte concentration inside the sensor and the bulk reservoir is weak. This leads to longer response times in the case of fast localized changes in concentration. However, for typical sensor designs, this effect impacts sensing performance on the millisecond scale and can be neglected in many applications. Experimentally, temporal sensing applicability for the detection of dopamine was recently confirmed and characterized in microfluidic environments (Kätelhön et al. 2010a,b).

Outlook and conclusions

We suppose that the recent concepts of nanocavity- and nanopore-based redox cycling sensors will receive growing attention during the next years and equally expect a steady increase in activity in this field of research.

On the one hand, the production method of these new types of sensors allows the fabrication of highly sensitive devices at comparably low fabrication costs and efforts. Contrasting IDAs, the inter-electrode distance is not limited by means of lateral structuring but only by the distance of an insulating layer. This can be easily downscaled to the nanometer level using low-cost and standard clean-room methods, hence, enabling ultra-high sensitivity. Also, the required structuring methods are limited to solely optical lithography, which is widely available in research and industry.

On the other hand, we adopt the view that current research on nanocavity and nanopore devices just started to pioneer a wide range of potential future applications. Particularly, with regard to biosensing, spectroscopic electro-analysis, as well as applications in neuroscience, we see an enormous potential that is still waiting to be explored. We further expect advances in theory and simulation science that provide new impulses to the development of novel spectroscopic applications.

Acknowledgments

We gratefully acknowledge funding by the Helmholtz Young Investigators Program.

References

Amatore, C.; Maisonhaute, E.; Simonneau, G. Ultrafast cyclic voltammetry: performing in the few megavolts per second range without ohmic drop. *Electrochem. Commun.* **2000**, *2*, 81–84.

Anderson, L. B.; Reilley, C. N. Thin-layer electrochemistry: steady-state methods of studying rate processes. *J. Electroanal. Chem.* **1965**, *10*, 295–305.

Aoki, K.; Morita, M.; Niwa, O.; Tabei, H. Quantitative analysis of reversible diffusion-controlled currents of redox soluble species at interdigitated array electrodes under steady-state conditions. *J. Electroanal. Chem.* **1988**, *256*, 269–282.

Bard, A. J.; Crayston, J. A.; Kittlesen, G. P.; Varco Shea, T.; Wrighton, M. S. Digital simulation of the measured electrochemical response of reversible redox couples at microelectrode arrays: consequences arising from closely spaced ultramicroelectrodes. *Anal. Chem.* **1986**, *58*, 2321–2331.

Bard, A. J.; Fan, F. R. F.; Kwak, J.; Lev, O. Scanning electrochemical microscopy. Introduction and principles. *Anal. Chem.* **1989**, *61*, 132–138.

Barker, A. L.; Gonsalves, M.; Macpherson, J. V.; Slevin, C. J.; Unwin, P. R. Scanning electrochemical microscopy: beyond the solid/liquid interface. *Anal. Chim. Acta* **1999**, *385*, 223–240.

Bledsoe, J. M.; Kimble, C. J.; Covey, D. P.; Blaha, C. D.; Agnesi, F.; Mohseni, P.; Whitlock, S.; Johnson, D. M.; Horne, A.; Bennet, K. E.; Lee, K. H.; Garris, P. A. Development of the wireless instantaneous neurotransmitter concentration system for intraoperative neurochemical monitoring using fast-scan cyclic voltammetry. *J. Neurosurg*. **2009**, *111*, 712–723.

Chidsey, C. E.; Feldman, B. J.; Lundgren, C.; Murray, R. W. Micrometer-spaced platinum interdigitated array electrode: fabrication, theory, and initial use. *Anal. Chem.* **1986**, *58*, 601–607.

Dam, V. A. T.; Olthuis, W.; van den Berg, A. Redox cycling with facing interdigitated array electrodes as a method for selective detection of redox species. *Analyst* **2007**, *132*, 365.

Engstrom, R. C.; Weber, M.; Wunder, D. J.; Burgess, R.; Winquist, S. Measurements within the diffusion layer using a microelectrode probe. *Anal. Chem.* **1986**, *58*, 844–848.

Engstrom, R. C.; Meaney, T.; Tople, R.; Wightman, R. M. Spatiotemporal description of the diffusion layer with a microelectrode probe. *Anal. Chem.* **1987**, *59*, 2005–2010.

Fan, F.-R. F.; Bard, A. J. Electrochemical detection of single molecules. *Science* **1995**, *267*, 871–874.

Feldman, B. J.; Murray, R. W. Measurement of electron diffusion coefficients through Prussian Blue electroactive films electrodeposited on interdigitated array platinum electrodes. *Anal. Chem.* **1986**, *58*, 2844–2847.

Goluch, E.; Wolfrum, B.; Singh, P.; Zevenbergen, M.; Lemay, S. Redox cycling in nanofluidic channels using interdigitated electrodes. *Anal. Bioanal. Chem.* **2009**, *394*, 447–456.

Henry, C. S.; Fritsch, I. Microcavities containing individually addressable recessed microdisk and tubular nanoband electrodes. *J. Electrochem. Soc.* **1999a**, *146*, 3367–3373.

Henry, C. S.; Fritsch, I. Microfabricated recessed microdisk electrodes: characterization in static and convective solutions. *Anal. Chem.* **1999b**, *71*, 550–556.

Hernández, G.; Shizgal, P. Dynamic changes in dopamine tone during self-stimulation of the ventral tegmental area in rats. *Behav. Brain Res.* **2009**, *198*, 91–97.

Honda, N.; Emi, K.; Katagiri, T.; Irita, T.; Shoji, S.; Sato, H.; Homma, T.; Osaka, T.; Saito, M.; Mizuno, J.; Wada, Y. 3-D comb electrodes for amperometric immuno sensors. *Transducers 03* **2003**, *2*, 1132–1135.

Howell, J. O.; Wightman, R. M. Ultrafast voltammetry and voltammetry in highly resistive solutions with microvoltammetric electrodes. *Anal. Chem.* **1984**, *56*, 524–529.

Huang, C.-W.; Lu, M. S.-C. Electrochemical detection of the neurotransmitter dopamine by nanoimprinted sub-microelectrodes and CMOS circuitry with near 100% collection efficiency. *Procedia Engineering* **2010**, *5*, 1196–1199.

Hüske, M.; Wolfrum, B. Fabrication of a nanoporous dual-electrode system for electrochemical redox cycling. *Phys. Status Solidi A* **2011**, *208*, 1265–1269.

Ino, K.; Saito, W.; Koide, M.; Umemura, T.; Shiku, H.; Matsue, T. Addressable electrode array device with IDA electrodes for high-throughput detection. *Lab Chip* **2011**, *11*, 385–388.

Kätelhön, E.; Hofmann, B.; Banzet, M.; Offenhäusser, A.; Wolfrum, B. Time-resolved mapping of neurotransmitter fluctuations by arrays of nanocavity redox-cycling sensors. *Procedia Engineering* **2010a**, *5*, 956–958.

Kätelhön, E.; Hofmann, B.; Lemay, S. G.; Zevenbergen, M. A. G.; Offenhäusser, A.; Wolfrum, B. Nanocavity redox cycling sensors for the detection of dopamine fluctuations in microfluidic gradients. *Anal. Chem.* **2010b**, *82*, 8502–8509.

Keithley, R. B.; Takmakov, P.; Bucher, E. S.; Belle, A. M.; Owesson-White, C. A.; Park, J.; Wightman, R. M. Higher sensitivity dopamine measurements with faster-scan cyclic voltammetry. *Anal. Chem.* **2011**, *83*, 3563–3571.

Kim, S. K.; Hesketh, P. J.; Li, C.; Thomas, J. H.; Halsall, H. B.; Heineman, W. R. Fabrication of comb interdigitated electrodes array (IDA) for a microbead-based electrochemical assay system. *Biosens. Bioelectron.* **2004**, *20*, 887–894.

Kraft, J. C.; Osterhaus, G. L.; Ortiz, A. N.; Garris, P. A.; Johnson, M. A. In vivo dopamine release and uptake impairments in rats treated with 3-nitropropionic acid. *Neuroscience* **2009**, *161*, 940–949.

Liu, H. Y.; Fan, F. R. F.; Lin, C. W.; Bard, A. J. Scanning electrochemical and tunneling ultramicroelectrode microscope for high-resolution examination of electrode surfaces in solution. *J. Am. Chem. Soc.* **1986**, *108*, 3838–3839.

Lohmüller, T.; Müller, U.; Breisch, S.; Nisch, W.; Rudorf, R.; Schuhmann, W.; Neugebauer, S.; Kaczor, M.; Linke, S.; Lechner, S.; Spatz, J.; Stelzle, M. Nano-porous electrode systems by colloidal lithography for sensitive electrochemical detection: fabrication technology and properties. *J. Micromech. Microeng.* **2008**, *18*, 115011.

McCarty, G. S.; Moody, B.; Zachek, M. K. Enhancing electrochemical detection by scaling solid state nanogaps. *J. Electroanal. Chem.* **2010**, *643*, 9–14.

Mirkin, M. V.; Horrocks, B. R. Electroanalytical measurements using the scanning electrochemical microscope. *Anal. Chim. Acta* **2000**, *406*, 119–146.

Neugebauer, S.; Müller, U.; Lohmüller, T.; Spatz, J. P.; Stelzle, M.; Schuhmann, W. Characterization of nanopore electrode structures as basis for amplified electrochemical assays. *Electroanalysis* **2006**, *18*, 1929–1936.

Neugebauer, S.; Stoica, L.; Guschin, D.; Schuhmann, W. Redox-amplified biosensors based on selective modification of nanopore electrode structures with enzymes entrapped within electrodeposition paints. *Microchim. Acta* **2008**, *163*, 33–40.

Nicholson, R. S. Theory and application of cyclic voltammetry for measurement of electrode reaction kinetics. *Anal. Chem.* **1965**, *37*, 1351–1355.

Nicholson, R. S.; Shain, I. Theory of stationary electrode polarography. Single scan and cyclic methods applied to reversible, irreversible, and kinetic systems. *Anal. Chem.* **1964**, *36*, 706–723.

Niwa, O. Electroanalysis with interdigitated array microelectrodes. *Electroanalysis* **1995**, *7*, 606–613.

Niwa, O.; Morita, M.; Tabei, H. Electrochemical behavior of reversible redox species at interdigitated array electrodes with different geometries: consideration of redox cycling and collection efficiency. *Anal. Chem.* **1990**, *62*, 447–452.

Oglesby, D. M.; Omang, S. H.; Reilley, C. N. Thin layer electrochemical studies using controlled potential or controlled current. *Anal. Chem.* **1965**, *37*, 1312–1316.

Rassaei, L.; Singh, P. S.; Lemay, S. G. Lithography-based nanoelectrochemistry. *Anal. Chem.* **2011**, *83*, 3974–3980.

Sanderson, D. G.; Anderson, L. B. Filar electrodes: steady-state currents and spectroelectrochemistry at twin interdigitated electrodes. *Anal. Chem.* **1985**, *57*, 2388–2393.

Shoup, D.; Szabo, A. Chronoamperometric current at finite disk electrodes. *J. Electroanal. Chem. Interfacial Electrochem.* **1982**, *140*, 237–245.

Singh, P. S.; Chan, H.-S. M.; Kang, S.; Lemay, S. G. Stochastic amperometric fluctuations as a probe for dynamic adsorption in nanofluidic electrochemical systems. *J. Am. Chem. Soc.* **2011**, *133*, 18289–18295.

Swamy, B. E. K.; Venton, B. J. Carbon nanotube-modified microelectrodes for simultaneous detection of dopamine and serotonin in vivo. *Analyst* **2007**, *132*, 876.

Takeda, M.; Shiku, H.; Ino, K.; Matsue, T. Electrochemical chip integrating scalable ring-ring electrode array to detect secreted alkaline phosphatase. *Analyst* **2011**, *136*, 4991–4996

Ueno, K.; Hayashida, M.; Ye, J.-Y.; Misawa, H. Fabrication and electrochemical characterization of interdigitated nanoelectrode arrays. *Electrochem. Commun.* **2005**, *7*, 161–165.

Vandaveer, W. R.; Woodward, D. J.; Fritsch, I. Redox cycling measurements of a model compound and dopamine in ultrasmall volumes with a self-contained microcavity device. *Electrochim. Acta* **2003**, *48*, 3341–3348.

Wightman, R. M. Probing cellular chemistry in biological systems with microelectrodes. *Science* **2006**, *311*, 1570–1574.

Wightman, R. M.; Jankowski, J. A.; Kennedy, R. T.; Kawagoe, K. T.; Schroeder, T. J.; Leszczyszyn, D. J.; Near, J. A.; Diliberto, E. J.; Viveros, O. H. Temporally resolved catecholamine spikes correspond to single vesicle release from individual

chromaffin cells. *Proc. Natl. Acad. Sci. USA* **1991**, *88*, 10754–10758.

Wolfrum, B.; Zevenbergen, M.; Lemay, S. Nanofluidic redox cycling amplification for the selective detection of catechol. *Anal. Chem.* **2008**, *80*, 972–977.

Zachek, M. K.; Takmakov, P.; Park, J.; Wightman, R. M.; McCarty, G. S. Simultaneous monitoring of dopamine concentration at spatially different brain locations in vivo. *Biosens. Bioelectron*. **2010**, *25*, 1179–1185.

Zevenbergen, M. A. G.; Krapf, D.; Zuiddam, M. R.; Lemay, S. G. Mesoscopic concentration fluctuations in a fluidic nanocavity detected by redox cycling. *Nano Lett.* **2007**, *7*, 384–388.

Zevenbergen, M. A. G.; Singh, P. S.; Goluch, E. D.; Wolfrum, B.; Lemay, S. G. Electrochemical correlation spectroscopy in nanofluidic cavities. *Anal. Chem.* **2009a**, *81*, 8203–8212.

Zevenbergen, M. A. G.; Wolfrum, B.; Goluch, E. D.; Singh, P. S.; Lemay, S. G. Fast electron-transfer kinetics probed in nanofluidic channels. *J. Am. Chem. Soc.* **2009b**, *131*, 11471–11477.

Zevenbergen, M. A. G.; Singh, P. S.; Goluch, E. D.; Wolfrum, B.; Lemay, S. G. Stochastic sensing of single molecules in a nanofluidic electrochemical device. *Nano Lett.* **2011**, *11*, 2881–2886.

Zhan, F.; Kuo, L.; Wang, S.; Lu, M. S.-C.; Chang, W.; Lin, C.; Yang, Y. An electrochemical dopamine sensor with CMOS detection circuit. *IEEE Sensors 2007 Conference* **2007**, 1448–1451.

Zhu, X. S.; Ahn, C. H. On-chip electrochemical analysis system using nanoelectrodes and bioelectronic CMOS chip. *IEEE Sensors Journal* **2006**, *6*, 1280–1286.

Zhu, X.; Ino, K.; Lin, Z.; Shiku, H.; Chen, G.; Matsue, T. Amperometric detection of DNA hybridization using a multi-point, addressable electrochemical device. *Sens. Actuators B* **2011**, *160*, 923–928.

Received November 10, 2011; accepted January 21, 2012; previously published online February 25, 2012

Enno Kätelhön studied Physics at RWTH Aachen, Germany, and extended his knowledge in nanoscience during an exchange to Delft University of Technology and Universiteit Leiden in the Netherlands. In 2007, he worked at SCHOTT North America in the field of Medical Imaging within the framework of an internship. Since 2010, he is following a PhD-program at Forschungszentrum Jülich GmbH at the Peter Grünberg Institute (PGI-8/ICS-8), where he focuses on the development of electrochemical devices for cell-chip communication.

Bernhard Wolfrum studied physics at the University of Göttingen, Germany, and at the University of California, Santa Barbara, USA. He did his PhD on shock waves and cavitation physics in Göttingen before working as a postdoc in the Institute of Bio- and Nanosystems at Forschungszentrum Jülich, Germany, and the Kavli Institute of Nanoscience at Delft University of Technology, The Netherlands. He is currently a Junior Professor at the RWTH Aachen and leader of a Helmholtz Young Investigator Group at the Peter Grünberg Institute, Forschungszentrum Jülich. His current research interest is directed at cell-chip communication with a focus on nanoscaled electrochemical interfaces.